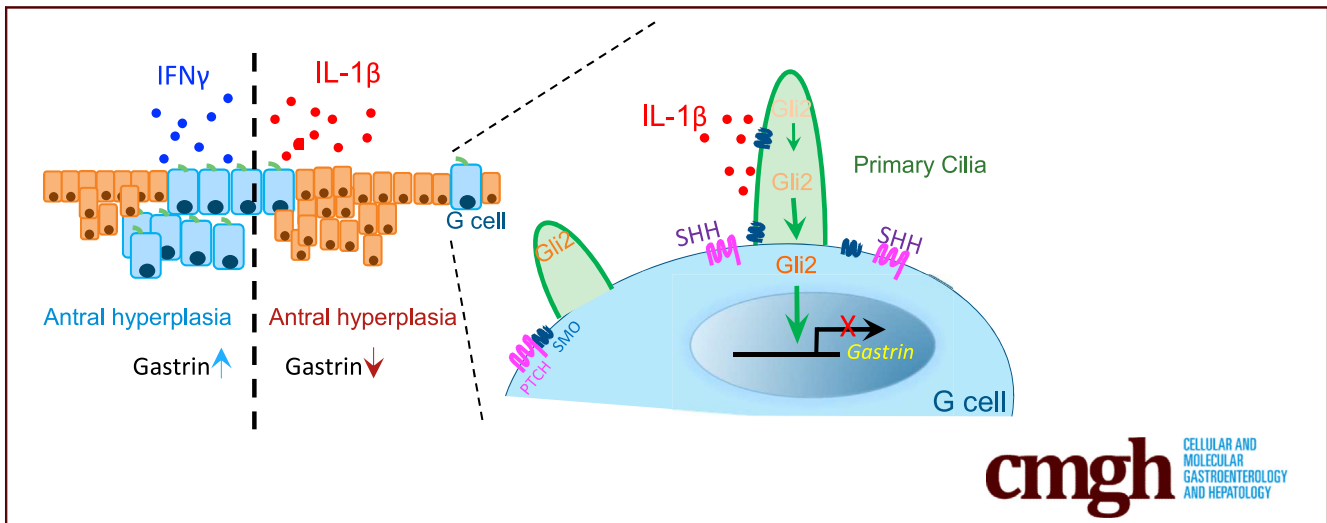


Interleukin-1 β Suppresses Gastrin via Primary Cilia and Induces Antral Hyperplasia



Lin Ding,^{1,2} Erica A. Sontz,² Milena Saqui-Salces,³ and Juanita L. Merchant^{1,2}

¹Department of Internal Medicine-Gastroenterology, University of Michigan, Ann Arbor, Michigan; ²Department of Medicine-Gastroenterology, University of Arizona, Tucson, Arizona; and ³Department of Animal Science, University of Minnesota, St. Paul, Minnesota



cmgh CELLULAR AND MOLECULAR GASTROENTEROLOGY AND HEPATOLOGY

SUMMARY

Transgenic expression of 2 common proinflammatory cytokines was directed to the mouse antrum. The prototypical Th1 cytokine interferon- γ stimulated gastrin and induced antral hyperplasia, whereas interleukin-1 β suppressed gastrin by releasing GLI2 from primary cilia, a hedgehog-regulated organelle and induced hyperplasia.

BACKGROUND & AIMS: *Helicobacter pylori* infection in humans typically begins with colonization of the gastric antrum. The initial Th1 response occasionally coincides with an increase in gastrin secretion. Subsequently, the gastritis segues to chronic atrophic gastritis, metaplasia, dysplasia and distal gastric cancer. Despite these well characterized clinical events, the link between inflammatory cytokines and non-cardia gastric cancer remains difficult to study in mouse models. Prior studies have demonstrated that overexpression of the Hedgehog (HH) effector GLI2 induces loss of gastrin (atrophy) and antral hyperplasia. To determine the link between specific cytokines, HH signaling and pre-neoplastic changes in the gastric antrum.

METHODS: Mouse lines were created to conditionally direct IL1 β or IFN- γ to the antrum using the *Gastrin-CreERT2* and Tet activator. Primary cilia, which transduces HH signaling, on G cells were disrupted by deleting the ciliary motor protein

KIF3a. Phenotypic changes were assessed by histology and western blots. A subclone of GLUTag enteroendocrine cells selected for gastrin expression and the presence of primary cilia was treated with recombinant SHH, IL1 β or IFN- γ with or without *kif3a* siRNA.

RESULTS: IFN- γ increased gastrin and induced antral hyperplasia. However, antral expression of IL1 β suppressed tissue and serum gastrin, while also inducing antral hyperplasia. IFN- γ treatment of GLUTag cells suppressed GLI2 and induced gastrin, without affecting cilia length. By contrast, IL1 β treatment doubled primary cilia length, induced GLI2 and suppressed gastrin gene expression. Knocking down *kif3a* in GLUTag cells mitigated SHH or IL1 β suppression of gastrin.

CONCLUSIONS: Overexpression of IL1 β in the antrum was sufficient to induce antral hyperplasia coincident with suppression of gastrin via primary cilia. ORCID: #0000-0002-6559-8184 (*Cell Mol Gastroenterol Hepatol* 2021;11:1251-1266; <https://doi.org/10.1016/j.jcmgh.2020.12.008>)

Keywords: *Helicobacter*; Hedgehog Signaling; IFN- γ ; Gastric Cancer; KIF3A.

More than half of the world's population is infected with *Helicobacter pylori* and approximately 1% of *H. pylori*-infected individuals progress to gastric cancer (GC), now the sixth most prevalent cancer worldwide.¹

Intestinal-type GCs typically arise in the distal stomach and were the third leading cause of cancer deaths until the discovery of *H pylori* and its treatment reduced their incidence.² *H pylori* typically colonizes the gastric antrum and initiates an intense Th1/Th17 inflammatory response that precedes gastric atrophy, intestinal metaplasia, and eventually cancer.³ Interleukin 1 β (IL1 β) and interferon- γ (IFN- γ) are 2 major proinflammatory cytokines that increase during *H pylori* infection, yet they seem to exhibit differential effects on the gastric mucosa.³ For example, IL1 β is a potent inhibitor of acid secretion and sonic hedgehog (SHH) signaling and acts as a driver of parietal cell atrophy.⁴ Patients exhibiting polymorphisms in the human IL1 β gene promoter are predisposed to developing GC.^{3,5} By contrast, the Th1 cytokine IFN- γ is a robust inducer of SHH.⁴ IFN- γ infusion stimulates gastrin and inhibits somatostatin, suggesting that it suppresses gastric atrophy.⁶ Ectopic expression of IL1 β or IFN- γ from parietal cells in the gastric corpus is sufficient to induce metaplastic changes.^{7,8} In contrast to humans, where *Helicobacter* typically colonizes the gastric antrum, mice exhibit corpus-dominant infection and inflammation with little antral involvement. A direct result of this observation is that prior mouse studies have not modeled the spectrum of GCs observed in human subjects, particularly in non-White populations who typically develop distal GC.^{9,10} Therefore, to address this gap in understanding, we generated 2 mouse models that directed the expression of these 2 proinflammatory cytokines to the antrum.

Helicobacter infection, chronic inflammation, and loss of SHH in the mouse corpus develops before parietal cell atrophy and a mucous cell type of metaplasia called spasmolytic polypeptide-expressing metaplasia (SPEM).^{11,12} Antral hyperplasia and subsequent tumor formation are primarily associated with inflammation and aberrant gastrin expression.^{13,14} Given its role in the gastric corpus,^{15,16} we queried as to whether HH signaling mediates inflammatory changes in the antrum. *Helicobacter* infection leads to a decrease in SHH expression in the corpus and this loss correlates with gastric atrophy and severe hypergastrinemia, suggesting a reciprocal relationship between gastrin and SHH. However, the mechanism of HH signaling in the antrum has been less defined during inflammatory conditions. Prior studies showed that increased IL1 β expression accompanies the development of antral tumors and induces expression of the hedgehog effector *Gli2* in epithelial cells.^{17,18} Ectopic *Gli2* expression in the antral mucosa induces antral tumors and directly suppresses gastrin by binding to its promoter.¹⁸ Vertebrate HH signaling depends on the presence of primary cilium, a highly specialized cellular organelle¹⁹ that retains GLI2 in the ciliary axoneme until the HH ligand engages its receptor PATCHED. Subsequently, activation of HH signaling prompts GLI2 movement to the cytoplasm where it is proteolytically processed before translocating to the nucleus. We previously reported that gastric endocrine cells exhibit primary cilia and speculated that these cilia mediate HH signaling in the antral G cell.²⁰ Because primary cilia have been implicated in several signaling pathways including HH and

IL1 β ,^{21,22} we assessed whether primary cilia on G cells modulate gastrin expression and contribute to preneoplastic changes in the antrum.


Results

Interferon- γ and Interleukin-1 β Induce Antral Hyperplasia But Exhibit Opposing Effects on Gastrin Expression

To model an intense proinflammatory response in the antrum, triple transgenic mouse lines were generated to overexpress IFN- γ or IL1 β in the presence of tamoxifen (TX) and doxycycline (DOX) (Figure 1A). Antral tissue levels of the 2 cytokines 8 weeks after DOX and TX treatment were elevated (Figure 1B and C). DOX treatment was administered in the drinking water to maintain transgene expression for 6 months. Blood via the submandibular vein was collected from live mice for serial determination of gastrin. Gastrin levels in the IL1 β -expressing mice decreased at 2 months and was significantly depressed after 5 months. In contrast, gastrin levels increased in the IFN- γ -expressing mice after 5 months (Figure 2A). However, despite their opposing effects on gastrin, both cytokines strongly induced epithelial cell hyperplasia in the antrum, with IL1 β overexpression causing a more aggressive change (Figure 2B). Overexpression of IFN- γ induced gastrin and chromogranin A expression in the antrum, but inhibited somatostatin expression in D cells, consistent with the expected feedback inhibition from gastrin.²³ Conversely, IL1 β suppressed gastrin, somatostatin, and chromogranin A expression demonstrating loss of the endocrine lineages (Figure 2B).

Along with hyperplastic changes in the antrum, SPEM was also observed in the corpus at 6 months following ectopic overexpression of IFN- γ or IL1 β (Figure 3A). SPEM development was determined by showing increased expression of Clusterin (SPEM marker), Trefoil factor 2 protein TFF2, and Griffonia simplicifolia lectin II (GS II) lectin (mucous neck cell marker), with a decrease in H⁺-K⁺-ATPase-expressing parietal cells. Coincident with gastrin suppression, we also found that IL1 β -overexpressing mice exhibited reduced gastric acidity compared with wild-type (WT) mice receiving the same treatment (Figure 3B and C). In addition, serum SHH levels were reduced with overexpression of IL1 β in the antrum. By contrast, gastric acidity in the IFN- γ -expressing mice increased, but did not reach statistical significance. Moreover, circulating SHH levels were not affected (Figure 3B and C).

Abbreviations used in this paper: DOX, doxycycline; ELISA, enzyme-linked immunosorbent assay; GC, gastric cancer; GLI2, glioma-associated oncogene family zinc finger 2; IFN- γ , interferon- γ ; IL1 β , interleukin-1 β ; KIF3A, Kinesin II family member 3A; qPCR, quantitative polymerase chain reaction; SHH, sonic hedgehog; SPEM, spasmolytic polypeptide-expressing metaplasia; Th1, T helper cell 1; TX, tamoxifen; dsddc1, wild-type C57BL/6 mice; WT, wild type.

 Most current article

© 2021 The Authors. Published by Elsevier Inc. on behalf of the AGA Institute. This is an open access article under the CC BY-NC-ND license (<http://creativecommons.org/licenses/by-nc-nd/4.0/>).

2352-345X

<https://doi.org/10.1016/j.jcmgh.2020.12.008>

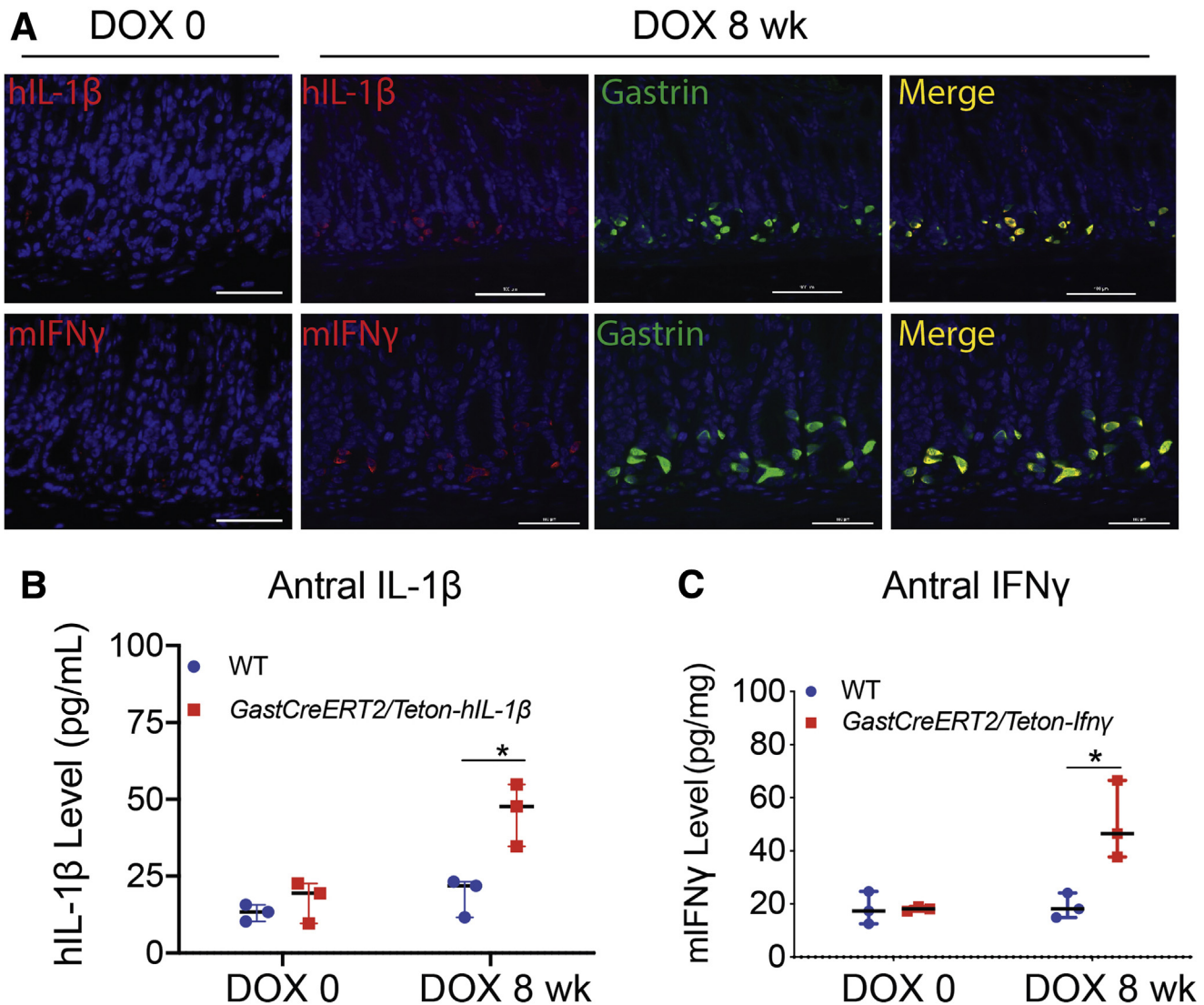


Figure 1. Characterization of *GastCreERT2/TetOn-mifn γ* and *GastCreERT2/TetOn-hIL1 β* triple transgenic mouse lines. Immunostaining for (A) human IL1 β (red) and mouse IFN- γ (red) colocalized with cells expressing gastrin (green) in the antrum of triple transgenic mice treated with tamoxifen before doxycycline (DOX 0) and after 8 weeks of tamoxifen and doxycycline treatment (DOX 8 weeks). Nuclei stained with DAPI (blue). Magnification $\times 400$. (B) Antral IL1 β and (C) IFN- γ were measured by ELISA. N = 3 mice. Horizontal lines represent the median and interquartile range. * $P < .05$.

Ectopic Expression of Sonic Hedgehog Induces GLI2 and Decreases Gastrin

To determine whether elevated levels of serum SHH suppress gastrin, we quantified the number of G cells (Figure 4A) in the antrum of mice overexpressing the SHH ligand (*pCMV-Shh*) at different time points after *Helicobacter felis* infection. We previously reported that *H felis* infection in the *pCMV-Shh* mouse generated 4-fold higher circulating levels of SHH compared with WT mice, and accelerated *H felis*-induced gastritis and SPEM development in the corpus.²⁴ The infected gastric antrum of *pCMV-Shh* mice did not exhibit significant epithelial or neoplastic changes but did show an increase in inflammatory cell infiltrates compared with infected WT antrum (Figure 4B). WT mice antra immunostained for gastrin showed twice as many G

cells per gland compared with uninfected and infected *pCMV-Shh* mice antra. *H felis* infection of WT or *pCMV-Shh* mice over 6 months did not change the number of G cells (Figure 4A). Although *H felis* infection increased circulating gastrin levels in WT mice, gastrin levels in the *pCMV-Shh* mice were significantly lower than WT control subjects and did not increase after *H felis* infection (Figure 4C). Higher circulating levels of SHH also corresponded to higher tissue levels of SHH in the gastric antrum (Figure 4D). Because GLI2, but not GLI1 or GLI3, suppresses the gastrin promoter in vitro,¹⁸ we surmised that SHH signaling inhibits gastrin. This hypothesis is consistent with our prior observation that antral G cells exhibit primary cilia²⁰ and suggests that they are capable of responding directly to the SHH ligand. Accordingly, we showed that ectopic SHH expression

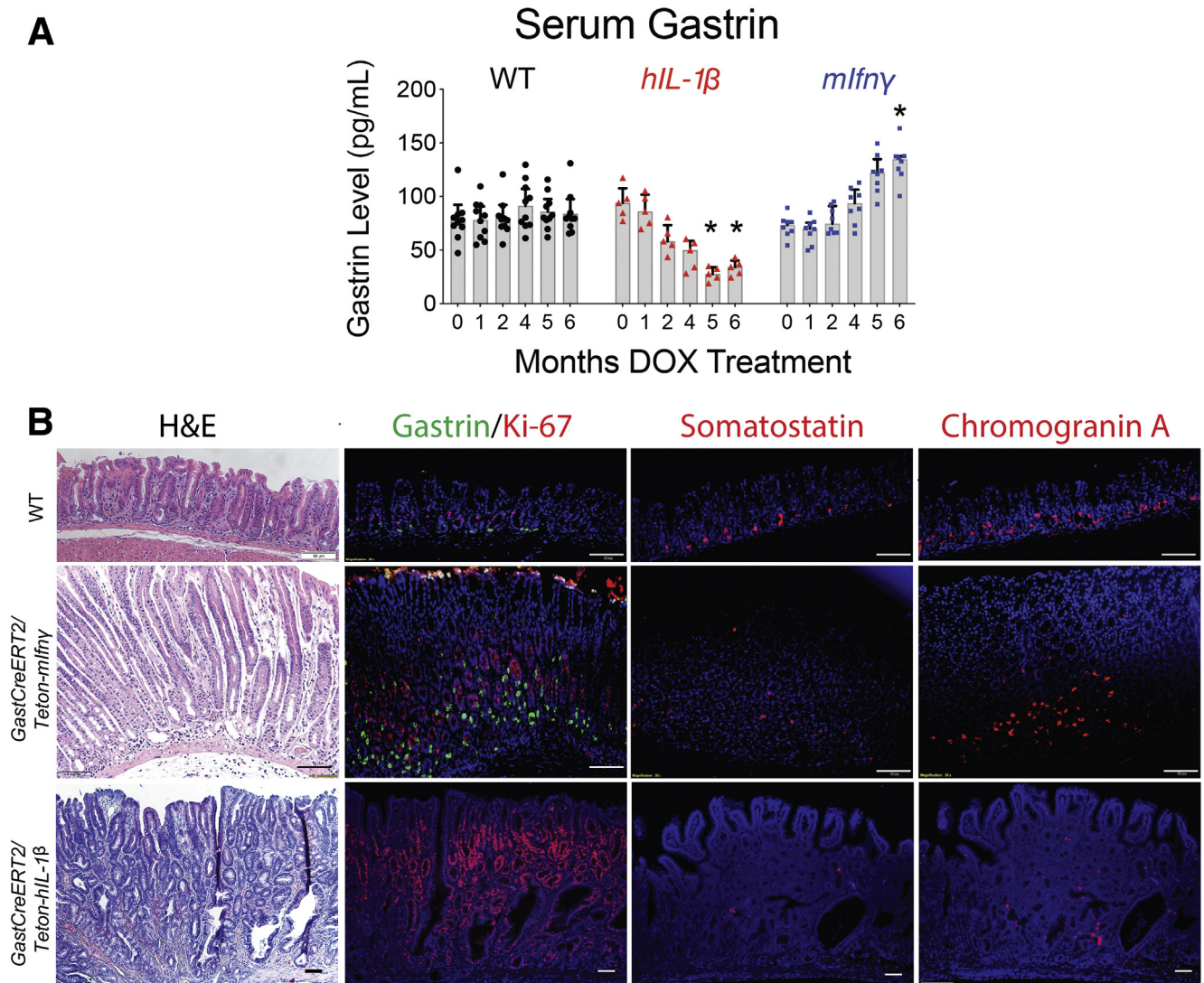


Figure 2. Overexpression of mIFN- γ or hIL-1 β in antral G cells induced antral hyperplasia and opposing effects on gastrin levels and endocrine cell lineage. *GastCreERT2/TetOn-mlfny* and *GastCreERT2/TetOn-hIL-1 β* mice were treated with tamoxifen and doxycycline for up to 6 months. (A) Serum gastrin levels were evaluated over time by ELISA. N = 5 mice per time point. * $P < .05$ relative to “0” time point. Horizontal lines represent the median and interquartile range. (B) Representative hematoxylin and eosin and immunofluorescent images of gastric antra immunostained for gastrin (green), Ki67 (red), somatostatin (red), and chromogranin A (red) for N = 3 mice. Nuclei stained with DAPI (blue). Scale bars = 50 μ m. H&E, hematoxylin and eosin.

initially increased GLI2 expression, which subsequently decreased over 6 months after *H felis* infection (Figure 4D). To assess whether there were qualitative differences in the inflammation, we quantified the levels of IFN- γ and IL1 β in the infected WT and *pCMV-Shh* mice and observed 2 distinct patterns. Serum levels of IFN- γ in both the WT and *pCMV-Shh* mice increased dramatically to the same level within 6 months, although the peak was delayed in the WT mice (Figure 4E). By contrast, IL1 β increased gradually in the WT mice but the anticipated increase was nearly 4-fold greater in the *pCMV-Shh* mice (Figure 4E). We also observed increased IL1 β -positive cells in the antrum of *pCMV-Shh* mice 6 months after the infection, whereas the number of IFN- γ -positive cells remained the same compared with the

WT-infected group (Figure 4E). Thus, HH signaling seemed to enhance the expansion of IL1 β -producing cells. Most of the IL1 β ⁺ cells (70%) are CD45⁺ leukocytes. There is also a small group of IL1 β ⁺ cells that are CD45-negative but E-cadherin-positive consistent with some epithelial cells expressing IL1 β (Figure 4F).

SHH is highly expressed in the gastric corpus especially in parietal cells.^{4,16} Conditional deletion of *Shh* or blocking HH signaling by overexpression of the HH inhibitor hedgehog-interacting protein-1 (HIP1) in parietal cells inhibits *H*, *K-ATPase* gene expression, acid secretion, and induces hypergastrinemia through a hypochlorhydric feedback mechanism.^{25,26} Moreover, cells in the deep antral gland also express SHH ligand, albeit at reduced

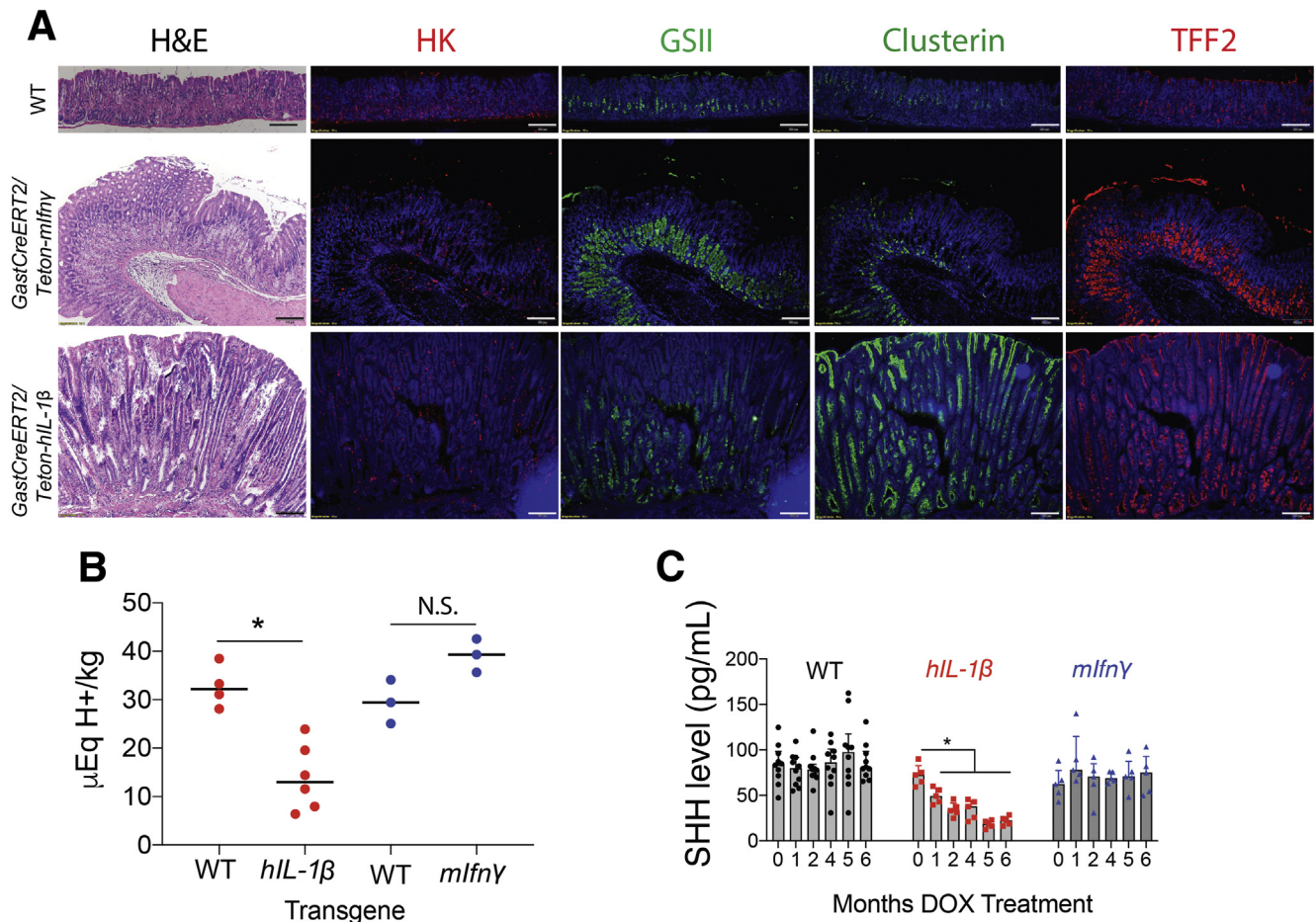


Figure 3. Effect of IL1 β and IFN- γ overexpression on cell composition of the gastric corpus, gastric acidity, and SHH ligand level. (A) Representative hematoxylin and eosin and immunofluorescent images of gastric corpus immunostained for GSII lectin (green), H⁺K⁺ATP4b (red), Clusterin (green), and TFF2 (red) for $n = 3$ mice. Nuclei stained with DAPI (blue). Scale bars = 100 μm . (B) Four months post tamoxifen and DOX treatment, the mice were necropsied, stomachs rinsed with 1.5 mL of saline for determination of gastric acidity by titration with 0.005 N sodium hydroxide. Gastric acidity was normalized to stomach weight. (C) Serum SHH levels were measured by ELISA. $N = 5\text{--}10$ mice per time point. * $P < .05$ compared with 0 time point. H&E, hematoxylin and eosin; N.S., not significant.

levels.^{15,16,18} Therefore, to rule out the possibility that antral inflammation stimulates the release of endogenous SHH in the antrum and mediates gastrin suppression, we deleted the *Shh* locus in antral G cells by breeding the *gast-creERT2* transgenic line to the *Shh^{FL/FL}* line (*Gast-CreERT2/Shh^{FL/FL}*). Unlike parietal cells, G cell-specific deletion of *Shh* had no significant effect on serum gastrin (Figure 5A–C), SHH peptide or HH signaling, specifically *Gli1* and *Gli2* mRNA (Figure 5D–F). Thus, we concluded that autocrine HH signaling does not contribute to the epithelial expression of GLI2 in G cells and subsequently suppression of gastrin gene expression.

Interleukin-1 β Induces GLI2-Mediated Suppression of Gastrin Through Primary Cilia

Although *Helicobacter* infection induces multiple proinflammatory cytokines, we found that IL1 β , in particular, modulates HH signaling and suppresses gastrin (Figure 2). To test this directly, we treated a subclone of GLUTag cells

that express gastrin and primary cilia with IL1 β (Figure 6). Primary cilia mediate HH signaling by restraining GLI2 until the HH ligand initiates signaling by engaging its receptor Patched.^{27,28} Because HH signaling also correlated with reduced gastrin, we queried whether the suppressive effect of IL1 β and HH signaling regulated antral G cells. Indeed IL1 β has been shown to regulate the HH effector GLI2¹⁸ and modulates nuclear factor- κ B and HIF2A via primary cilia,^{29,30} suggesting that this proinflammatory cytokine might converge with HH signaling at primary cilia. To test this concept further, we compared treatment of the SF9 GLUTag subclone with the 2 proinflammatory cytokines and found that IFN- γ increased release of gastrin peptide into the media by 2.5-fold, whereas IL1 β suppressed the release of gastrin by 50% (Figure 6A). The fluctuations in peptide levels corresponded to equivalent changes in *gastrin* mRNA. IFN- γ induced *gastrin* mRNA >10-fold, whereas IL1 β suppressed *gastrin* mRNA by at least 75% (Figure 6B). In addition, we observed an increase in GLI2 mRNA and protein levels by IL1 β , but IFN- γ had no effect on GLI2

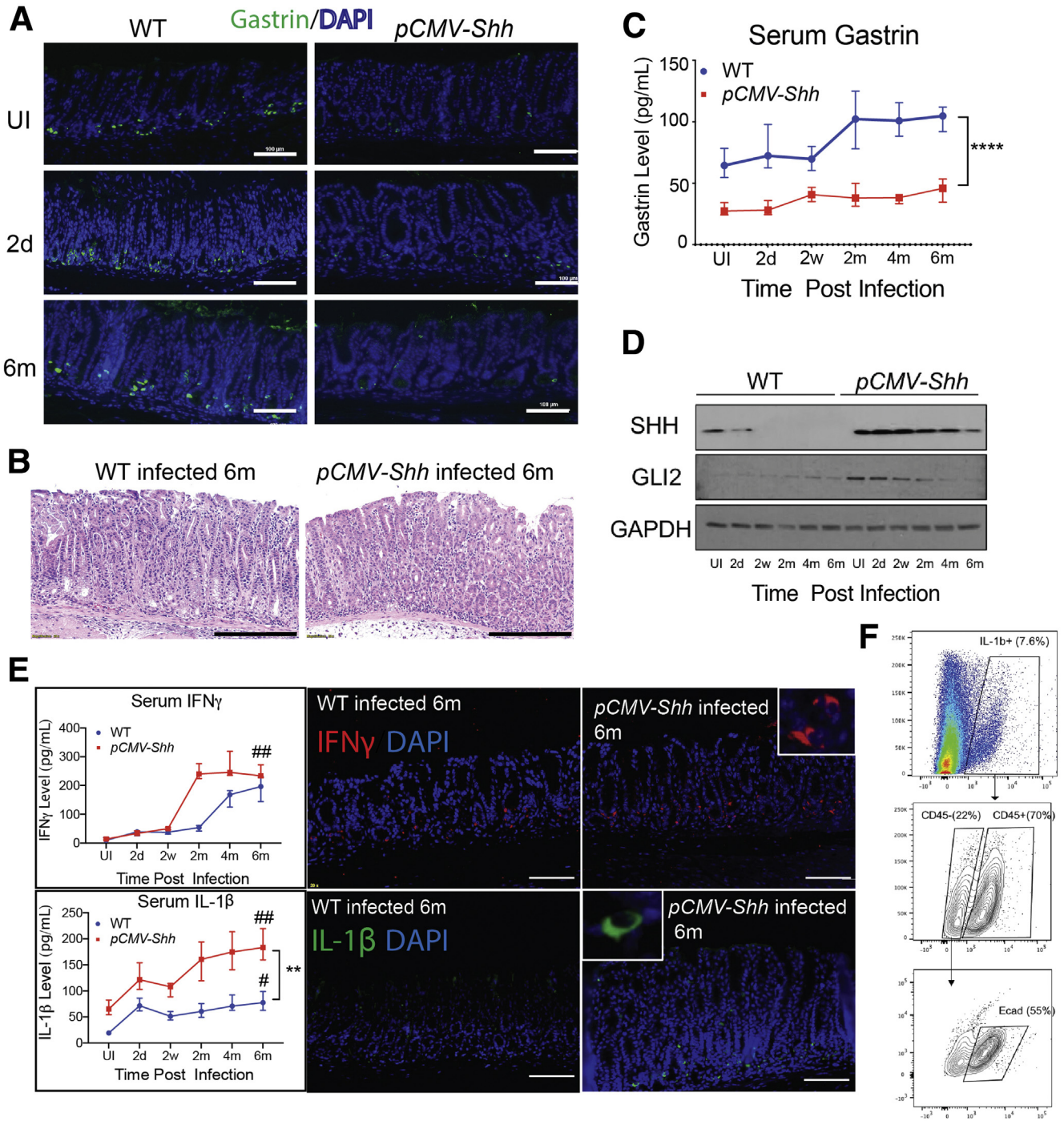


Figure 4. Ectopic SHH expression suppressed gastrin and induced GLI2 in the antrum during *Helicobacter felis* infection. Representative (A) immunofluorescent images of gastric antrum stained for gastrin (green) and (B) hematoxylin and eosin images at the indicated times postinfection. Scale bars = 100 μ m. (C) Serum gastrin levels were measured by ELISA. (D) The gastric antra were analyzed for GLI2, SHH (N-terminal peptide), and GAPDH protein by Western blot. (E) Serum IFN- γ and IL1 β levels were determined by ELISA and immunostaining in *Helicobacter*-infected gastric antrum. Nuclei stained with DAPI (blue). Scale bars = 50 μ m. Inset: magnification \times 1000. N = 8–10 mice per time point. Horizontal lines represent the median and interquartile range. ** P < .05 < .01; **** P < .0001, comparing WT versus pCMV-Shh mouse lines. # P < .05, ## P < .01, compared with the uninfected time point. (F) IL1 β -positive cells from the antrum were analyzed for CD45 and E-cadherin by flow cytometry. UI, uninfected time point.

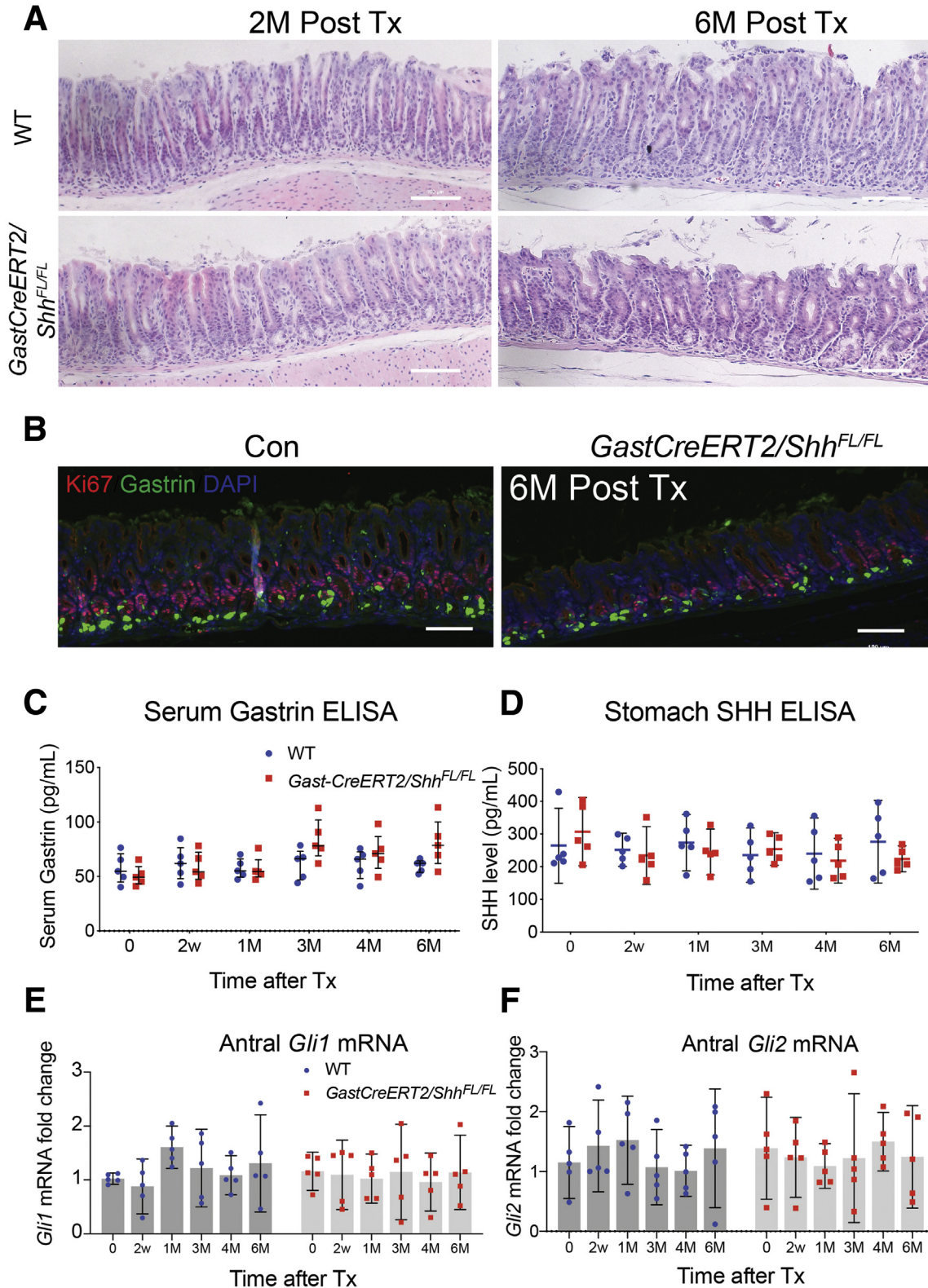


Figure 5. Deletion of SHH in the G cells does not modulate gastrin expression. Representative (A) hematoxylin and eosin images and (B) immunofluorescent images of gastric antrum stained with gastrin (green) and Ki67 (red) from WT and *Gast-CreERT2:Shh^{FL/FL}* mice at the indicated times post tamoxifen injection. Nuclei stained with DAPI (blue). Scale bars = 100 μ m. (C) Serum gastrin levels and (D) SHH levels in whole stomach were determined by ELISA. (E) *Gli1* mRNA and (F) *Gli2* mRNA in the antrum of WT and *GastCreERT2/Shh^{FL/FL}* mice were quantified by qPCR. N = 5 mice per time point. Horizontal lines represent the median and interquartile range.

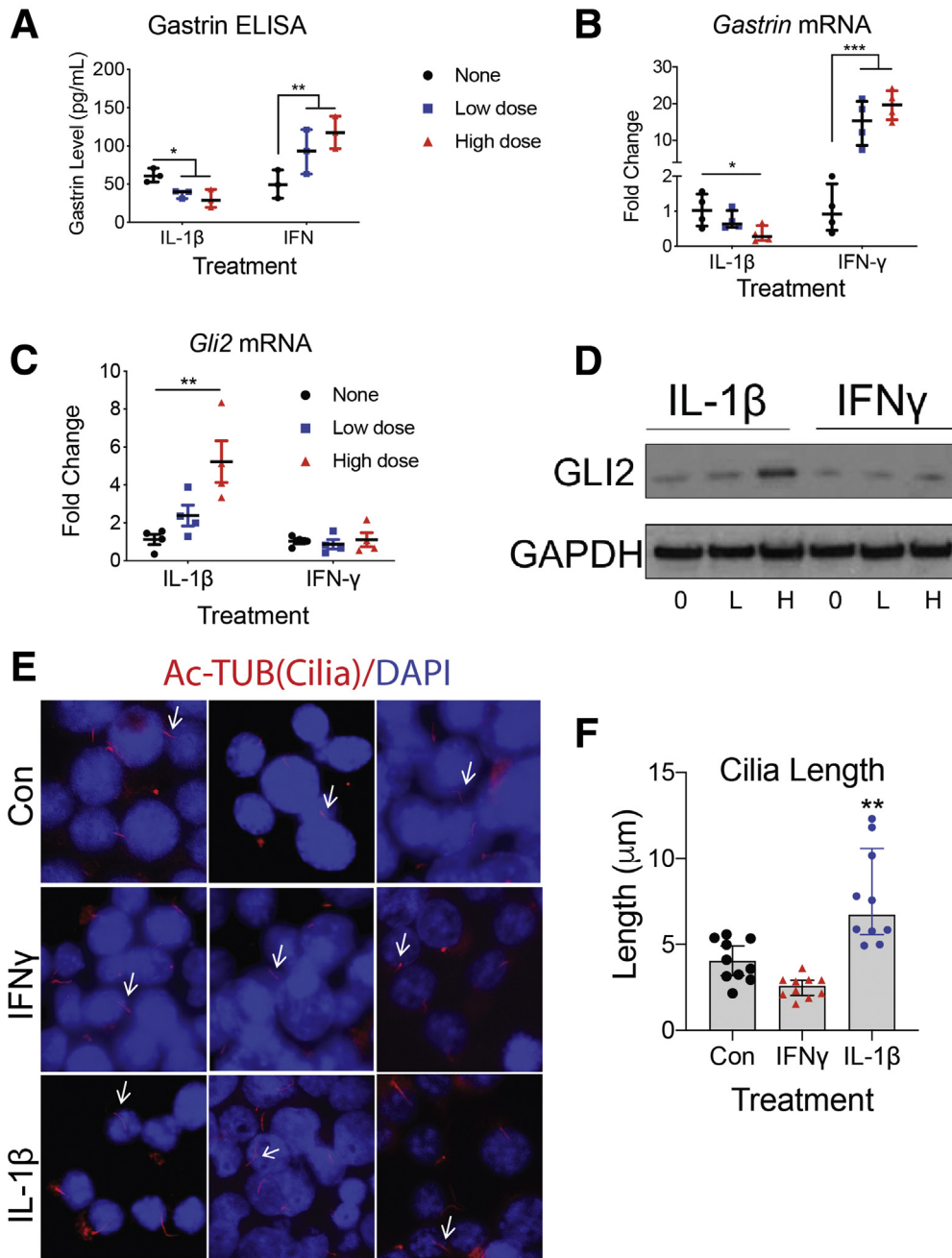


Figure 6. IL1 β elongates primary cilia and induces GLI2-mediated suppression of gastrin in GLUTag subclone cells. The SF9 subclone of GLUTag cells were treated with low (L, 5 ng/mL) or high (H, 10 ng/mL) doses of recombinant IL1 β or IFN- γ (L, 200 U/mL, H, 800 U/mL) for 24 hours. None = no treatment. n = 4 experiments. (A) Gastrin levels in conditioned media were determined by ELISA and (B) *Gastrin* mRNA in cell lysates was quantified by qPCR. (C) *Gli2* mRNA levels were quantified by qPCR and (D) GLI2 protein levels were determined by Western blot. (E) Axonemes of primary cilia (arrows) were identified by immunostaining for acetylated tubulin (Ac-TUB, red) on GLUTag cells treated with IFN- γ (800 U/mL) or IL1 β (10 ng/mL). (F) Mean cilium length was quantified using ImageJ. Ten images of randomly chosen areas at $\times 1000$ magnification were taken from each treatment for quantitation. Horizontal lines represent the median and interquartile range. * $P < .05$, ** $P < .01$, *** $P < .001$ relative to none or Con group.

(Figure 6C and D). Wann and Knight²¹ reported that IL1 β modulates cilia by increasing their length. Similarly, we found that recombinant IL1 β increased primary cilia length on GLUTag cells, whereas IFN- γ exerted no effect on cilia length (Figure 6E and F), suggesting that primary cilia lengthening corresponded to increased expression of GLI2. As observed in vitro, we also observed longer cilia on G cells in the antra of *GastCreERT2/TetOn-hIL-1 β* mice (Figure 7A). Western blot analysis of antral tissue from IL1 β -overexpressing mice confirmed an increase in GLI2 and the ciliary motor protein KIF3A, which is required for cilia formation (Figure 7B). This result was consistent with primary cilia serving as an important reservoir for GLI2. Thus,

we speculated that the increase in primary cilia length by IL1 β suppresses gastrin by activating GLI2. By contrast, IFN- γ overexpression suppressed GLI2 without any effect on primary cilia length (Figure 7B), suggesting that this cytokine regulated GLI2 and gastrin through a different signaling pathway.

Disrupting Primary Cilia on Gastrin-Expressing Cells Induces Gastrin Expression and Antral Hyperplasia

To determine if the SHH and IL1 β effect on gastrin gene expression required primary cilia, *kif3a* was knocked down

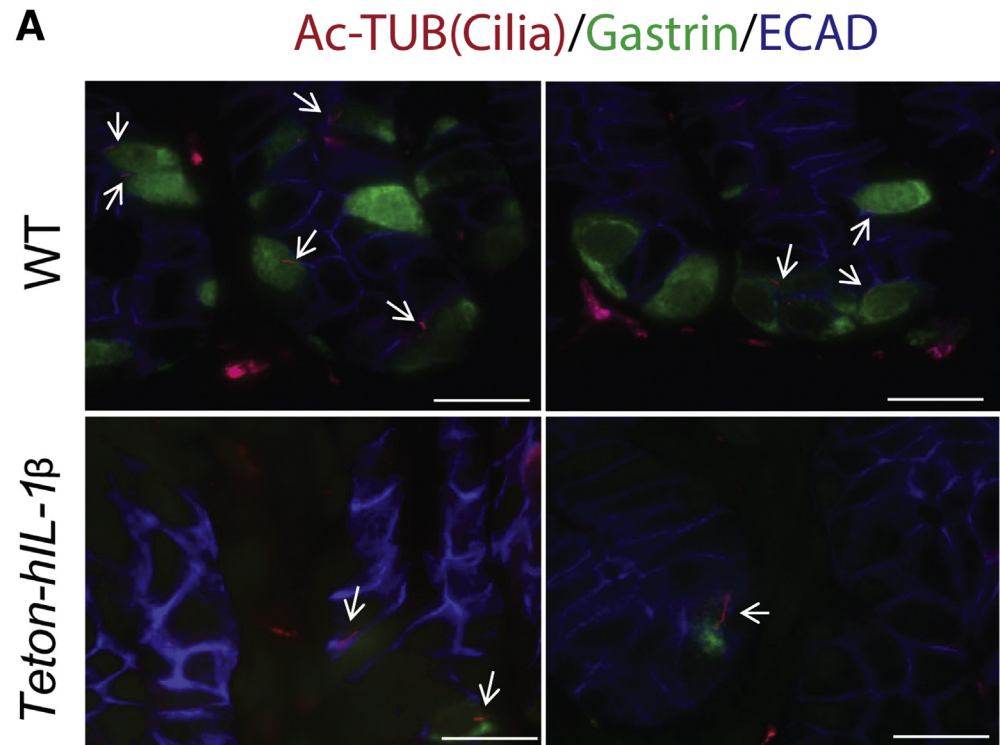
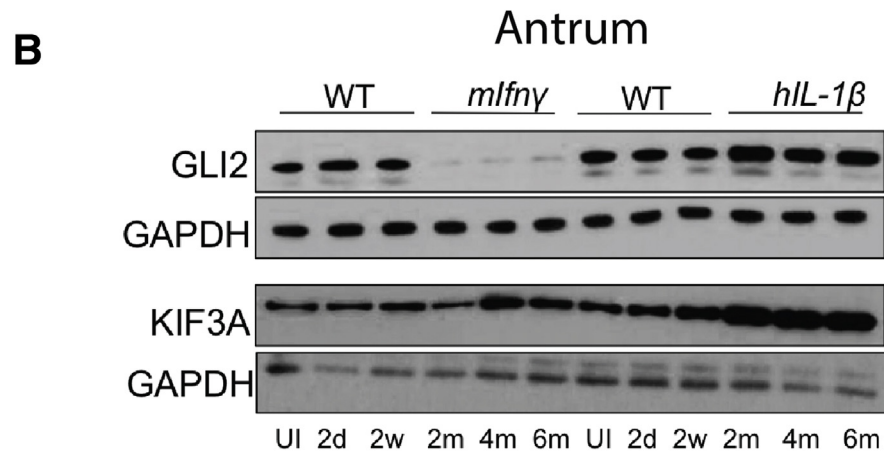


Figure 7. IL1 β over-expression elongates primary cilia and induces Gli2 in vivo. (A) Representative immunofluorescent images of the gastric antrum immunostained for primary cilia (Ac-Tub, red), gastrin (green), and E-cadherin (blue) from WT and *GastrinCreERT2/TetOn-hIL-1 β* mice. Cilia were identified in gastrin⁺ cells (arrows). Scale bars = 10 μ m. (B) The antrum was analyzed for GLI2, KIF3A, and GAPDH protein by Western blot. Shown are the levels in 3 mice per group, time point 6 months after tamoxifen treatment.



in the GLUTag cells (Figure 8A) to disrupt the presence of primary cilia (Figure 8B). SHH and IL1 β suppressed gastrin peptide secretion into the media by approximately 70%. However, knockdown of *kif3a* induced gastrin secretion compared with untreated cells and abolished the suppressive effect of SHH or IL1 β on gastrin (Figure 9A). *Gastrin* mRNA levels coincided with the changes in secreted gastrin peptide (Figure 9B). Therefore, primary cilia on gastrin-expressing enteroendocrine cells mediate IL1 β and HH signaling and in turn modulate gastrin expression and secretion.

To determine the role of primary cilia in vivo, primary cilia on G cells were disrupted by deleting *kif3a* (*Gast-CreERT2/kif3a^{FL/FL}*) (Figure 9C). Cell-specific deletion of

kif3a significantly increased serum gastrin levels over 7 months (Figure 9D). Immunohistochemical analysis revealed antral hyperplasia with a significant increase in the number of antral G cells (Figure 9E). Western blot analysis demonstrated a decrease in GLI2 protein with deletion of *kif3a* (Figure 9F). Therefore, G cell-specific disruption of primary cilia reduced the levels of the GLI2 transcriptional protein and abrogated its suppressive effect on gastrin gene expression.

Discussion

Much of the serious sequelae from chronic *H pylori* infections might be caused by an aberrant host immune

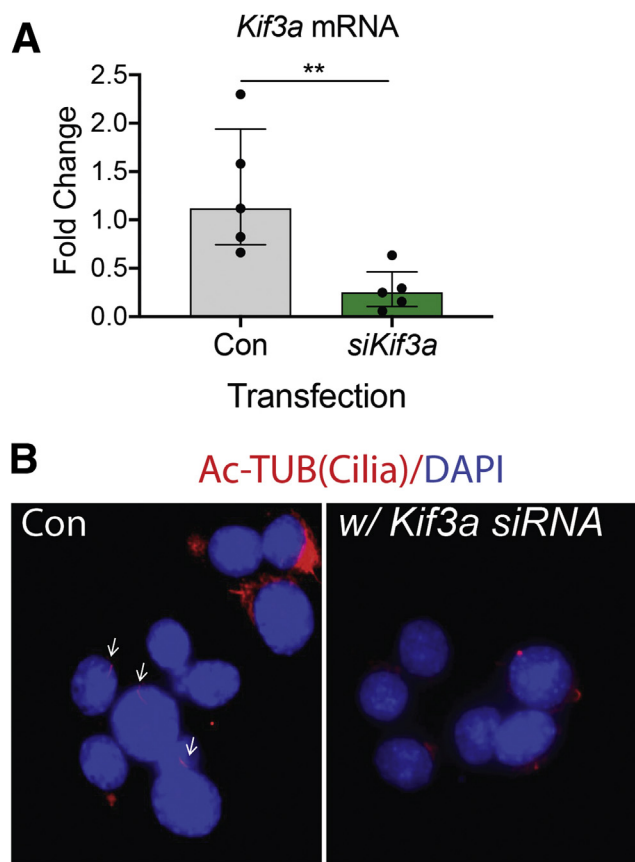


Figure 8. Validation of *Kif3a* siRNA knockdown in GLUTag cells. The SF9 GLUTag subclone was transfected with *Kif3a* siRNA to disrupt primary cilia or control siRNA. (A) *Kif3a* mRNA levels were determined by qPCR. $n = 5$ experiments. $**P < .01$. (B) Axonemes of primary cilia (arrows) were identified by immunostaining for acetylated tubulin (Ac-TUB, red). Magnification $\times 1000$.

response rather than from bacterial virulence factors.³¹ In an era of increasing *Helicobacter*-resistant strains and non-*Helicobacter*-mediated chronic atrophic gastritis,²³ it is important to increase the armamentarium of treatments to prevent or at least mitigate the inflammatory signals promoting gastric proliferation, dysplasia, and eventually transformation. We report here that at least 2 proinflammatory cytokines exert differential effects in the antrum. Although both are proinflammatory cytokines, IFN- γ stimulated gastrin and enhanced gastric acid secretion, whereas IL1 β suppressed G cells along with other endocrine cell types in the hyperplastic antrum.

Expression of GLI2 *in vivo* is sufficient to induce dysplastic tumors and even adenocarcinoma in the antrum.^{17,18} A striking feature of atrophy in the antrum is the loss of gastrin-expressing cells. In studies using transfected cell lines, GLI2 inhibited gastrin reporter activity and gastrin gene expression *in vitro*.¹⁸ Moreover *in vivo* expression of *Gli2* in *Lgr5*⁺ antral stem cells induces invasive adenocarcinomas.¹⁷ Here, we concluded that either *Helicobacter* infection or HH signaling can increase IL1 β expression and promote expression of the proto-oncogene

and hedgehog effector GLI2. In this manner, HH signaling components cooperate specifically with the proinflammatory cytokine IL1 β to suppress gastrin expression in the antrum.

Although IL1 β and IFN- γ are proinflammatory cytokines induced by *Helicobacter* infection, only IL1 β has been shown to modulate primary cilia, albeit on chondrocytes, by inhibiting histone deacetylase activity and subsequently increasing the pool of acetylated tubulin.^{21,32} We conclude from the studies here that IL1 β , like SHH ligand, mediates its suppressive effect on the antral G cell via primary cilia. Disruption of primary cilia using an epithelial Cre driver (*ShhCre*) resulted in G cell hyperplasia and sustained hypergastrinemia within weeks and subsequently corpus metaplasia by 7–8 months, but no antral hyperplasia was observed.²⁰ Importantly, the largest reservoir of SHH in the stomach is the parietal cell. Once corpus atrophy and metaplasia develops, SHH is likely not available to induce the hyperplastic changes observed in the antrum. Rather, chronic atrophic gastritis is more likely induced and sustained by IL1 β . Here we show that cell-specific disruption of cilia on antral G cells was sufficient to increase their numbers and gastrin secretion, which led to antral hyperplasia within 7 months. Therefore, primary cilia on G cells seems to regulate gastrin gene expression and secretion. We speculate that elongation of primary cilia in response to IL1 β might accelerate the anterograde intraflagellar transport thereby increasing delivery of ciliary components,^{33,34} which includes GLI2, a direct *gastrin* gene suppressor. By comparison, IFN- γ suppressed GLI2 and induced gastrin and antral hyperplasia, without affecting primary cilia length. This result might explain how chronic inflammation blocked induction of gastrin in the *pCMV-Shh* mice after 6 months of the *Helicobacter* infection. Indeed, disruption of another ciliary protein IFT88 blocks IL1 β inflammatory changes.³² Because the overexpression of proinflammatory cytokines also modulated expression of the hormone gastrin and other undetermined secreted products, the chronic effect of these cytokines on epithelial differentiation might be caused by these secondary changes.

In summary, our study provides evidence that both SHH and IL1 β signaling require primary cilia on G cells to modulate gastrin expression and antral transformation via GLI2. The study also demonstrates that not all proinflammatory cytokines exert the same effect on their cellular targets. Apparently, a combination of cytokines in various quantities is generated during a *Helicobacter* infection and can either synergize or oppose each other. Using a reductionist approach in which individual cytokines were expressed in a cell-specific manner, we isolated the differential effects of at least 2 proinflammatory cytokines. Because there is wide variability in how individuals respond to an *H pylori* infection, the study here provides new insights into how different proinflammatory cytokines might contribute to diverse outcomes. For example, it is not understood why some *H pylori*-infected subjects develop peptic ulcer disease, a high-gastrin state with increased gastric acidity, whereas others respond by developing gastric atrophy and metaplasia in the antrum, a low-gastrin and low-acid state. These differential

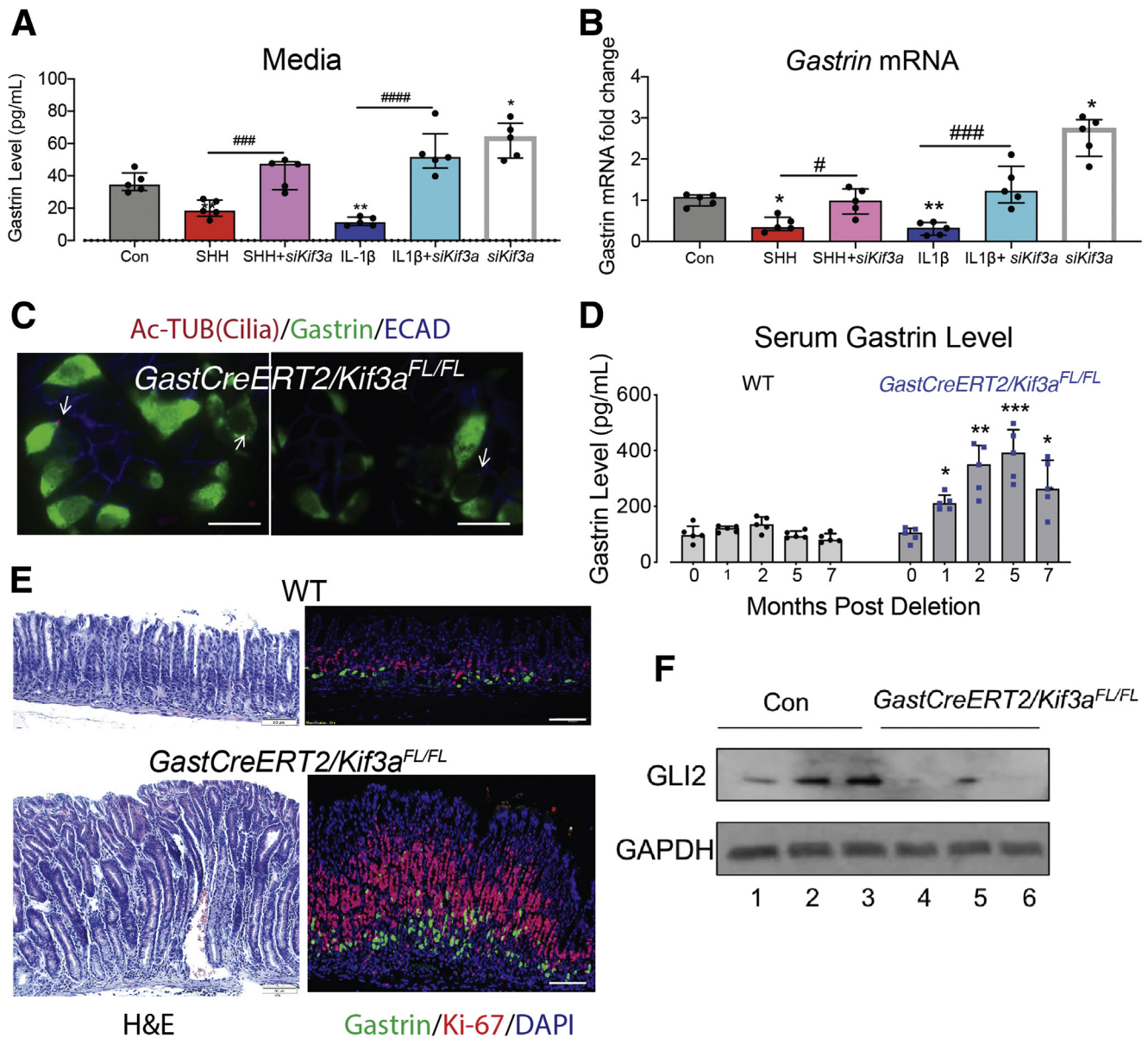


Figure 9. Disruption of primary cilia on gastrin-expressing cells induced gastrin expression and antral hyperplasia. SF9 GLUTag cells were transfected with *kif3a* siRNA to disrupt primary cilia and then treated with recombinant SHH (400 ng/mL) or IL1 β (10 ng/mL) for 24 hours. (A) Secreted gastrin peptide in conditioned media was determined by ELISA and (B) *Gastrin* mRNA levels were determined by qPCR. $n = 5$ experiments. $*P < 0.05$ relative to Con. $\#P < .05$, $###P < .001$, $####P < .0001$. Horizontal lines represent the median and interquartile range. Primary cilia on G cells were disrupted by deleting *kif3a* in *GastCreERT2/kif3a^{FL/FL}* mice for up to 7 months. (C) Axonemes of primary cilia (arrows) in *GastCreERT2/kif3a^{FL/FL}* mice were identified by immunostaining for acetylated tubulin (Ac-TUB, red) and colocalized with gastrin (green) and E-cadherin (blue). Scale bars = 10 μ m. (D) Serum gastrin levels were determined by ELISA over 7 months. $n = 5$ mice per time point. Horizontal lines represent the median and interquartile range. $*P < .05$, $**P < .01$, $***P < .001$ relative to time point 0. (E) Representative hematoxylin and eosin images and immunofluorescent images of gastric antrum stained with gastrin antibody (green). Scale bars = 50 μ m. (F) Antral GLI2 and GAPDH protein determined by Western blot. $n = 3$ mice per group at time point 7 months. H&E, hematoxylin and eosin.

responses to the inflammation need to be taken into consideration if novel treatments are developed for resistant *H pylori* infections or subjects who are *H pylori* negative, yet exhibit chronic atrophic gastritis and metaplasia at risk for progression to GC.

Materials and Methods

Transgenic Mice

All mouse lines were bred onto a C57BL/6 genetic background. The *pCMV-Shh* transgenic mouse line has been described previously.^{24,35} N-terminally HA-tagged Shh cDNA

were expressed from the CMV promoter. These mice have gastritis and infrequent metaplasia, and generated 4-fold higher circulating levels of SHH compared with WT mice. The University of Michigan Transgenic Mouse Recombinering Core generated the gastrinCreERT2 transgene (*GastCreERT2*) by inserting a *pCMVCreERT2* cassette into the second exon of a bacterial artificial chromosome containing the mouse gastrin gene (RP23-29313 clone purchased from BACPAC genomics, bacpacresources.org). The *GastCreERT2* transgenic mouse line was bred to the *ROSA26-LSL-CAG-tdTomato* line (Jackson Labs, #007914) and the hybrid line was treated with TX. *GastCreERT2* cell-specific expression was confirmed by costaining frozen sections with gastrin antibody (Figure 10). After confirming cell-specific expression, the *GastCreERT2* line was then bred to the *rtTA* mouse line (*ROSA26-CAG-LSL-rtTA*, Jackson Labs #029617), which expresses the Tet activator (rtTA) on removal of the stop codon by the Cre recombinase. We subcloned the human *IL1 β* cDNA (IMAGE Clone 3875593) into the *HindIII* site of *pTetSplice* downstream of the *Tet Operon* binding sites (*pTetO-hIL-1 β*). The construct was genotyped using the primer pairs: forward 5'-CAGTGCCACGTTGTGAGTTG-3'; reverse 5'-GGTCGGAGATTCGTAGCTGG-3'. A similar construct was generated by subcloning the mouse *Ifn γ* cDNA (IMAGE Clone 8733812) into the *HindIII* site of *pTetSplice* (*pTetO-mlfn γ*),⁸ which was genotyped using the primer pairs: forward 5'-CGAATTCGAGCTCGG TACCC-3'; reverse 5'-CCATCCTTTGCCAGTTCCTCCAG-3'. Mouse lines were generated using the *pTetO-hIL-1 β* and *pTetO-mlfn γ* plasmids and then were bred to the hybrid mouse line expressing *GastCreERT2;R26-LSL-rtTA*. Inducible G cell-specific overexpression of the 2 cytokines was achieved by intraperitoneally injecting the triple transgenic mice (at 6–8 weeks of age) expressing *GastCreERT2; R26-LSL-rtTA;pTetO-hIL-1 β* or *pTetO-IFN γ* with TX (0.2 mg/g body weight) for 5 consecutive days and then 1 injection each of the following months. In addition, DOX (2 mg/mL of water) was administered in the drinking water every day until euthanized (Figure 11). Conditional deletion of *Kif3a* or *Shh* was achieved by crossing *Kif3a^{tm2.1Gsn/+}* mice³⁶ or *Shh^{Fl/Fl}* mice²⁶ to *GastCreERT2* mice. *Kif3a^{tm2.1Gsn/+}* mice were genotyped using the primer pairs: forward 5'-AGGGCA GACGAAGGGTGG-3'; reverse 5'-TCTGTGAGTTTGTGAC-CAGCC-3'. *Shh^{Fl/Fl}* mice were genotyped using the primer pairs: forward 5'-ATGCTGGCTCGCCTGGCTGTGG AA-3'; reverse 5'-GAAGAGATCAAGCAAGCTCTGGC-3'. To conditionally delete *Kif3a* or *Shh*, mice (at 6–8 weeks of age) were intraperitoneally injected with TX (0.2 mg/g body weight) for a week and then once each month until euthanized.

All mice were housed under the same specific pathogen-free conditions and fasted overnight before euthanasia with free access to water. The University of Michigan and University of Arizona Institutional Animal Care and Use Committees approved all mouse protocols used in this study.

Cell Culture

The GLUTag murine enteroendocrine cell line was generated from a colonic tumor that developed in mice

expressing the SV40 large T antigen (Tag) from the glucagon promoter.³⁷ Using single cell culture, we identified a subclone of GLUTag cells (SF9) that express primary cilia and high levels of gastrin peptide. For maintenance, cells were grown in DMEM (5.6 mmol/L glucose) supplemented with 10% fetal bovine serum, 2 mmol/L L-glutamine, 100 IU/mL penicillin, and 100 μ g/mL streptomycin. Following serum starvation for 24 hours, the SF9 GLUTag subclone at 40%–60% confluency was treated with low-dose (5 ng/mL) or high-dose (10 ng/mL) IL1 β (#50101-MNAE, SinoBiological, Chesterbrook, PA); low-dose (200 U/mL) or high-dose (800 U/mL) IFN- γ (#PMC4031, Thermo Fisher, Waltham, MA), or SHH (#461-SH/CF, 400 ng/mL, R&D, Minneapolis, MN) for 24 hours before collecting conditioned media for enzyme-linked immunosorbent assay (ELISA). *Kif3a* siRNA or the scrambled controls were transfected using Lipofectamine RNAiMAX transfection reagent (Thermo Fisher) for 48 hours before cytokine treatment. *Kif3a* knockdown was validated by quantitative polymerase chain reaction (qPCR) and presence of primary cilia determined by acetylated-tubulin (Ac-tub) staining.

Helicobacter felis Culture and Infection

H felis (CS1 strain) were cultured in sterile-filtered Brucella broth medium (BD, Franklin Lakes, NJ) plus 10% horse serum (Atlanta Biologicals, Lawrenceville, GA) using the GasPak EZ Campy Container System (BD) at 37°C with shaking at 100 rpm. The bacterial culture suspension was collected by centrifuging at 1400 $\times g$ in a Beckman Allegra X-30r centrifuge at room temperature. Subsequently the bacterial pellets were resuspended in saline solution. Optical density of the resuspended *H felis* was determined and the final concentration was adjusted to 10⁹ *H felis* cells in 1 mL saline. Mice were gavaged once a day with 10⁸ *H felis* CFUs in 100 μ L saline for 3 consecutive days. Control mice were gavaged with 100 μ L of saline solution.

Tissue Preparation

Mice were fasted for 16 hours before being euthanized. The forestomach was removed before bisecting the stomach along the greater and lesser curvatures then sectioning each half into longitudinal strips. Tissue strips were fixed overnight in 10% formalin and transferred to 70% ethanol for subsequent paraffin embedding. Some corpus or antral tissue was minced for total RNA and protein analysis.

Enzyme-Linked Immunosorbent Assay

Mice were fasted for 16 hours before serial collection of blood via submandibular vein phlebotomy. Serum was obtained by centrifugation at 1000 $\times g$ for 15 minutes at room temperature. Tissue protein was extracted by homogenizing gastric tissue in RIPA buffer supplemented with protease inhibitors (Thermo Fisher, #78425). The supernatant was used for tissue ELISAs. Gastrin levels were determined using the Human/Mouse/Rat Gastrin-I Enzyme Immunoassay Kit (RayBiotech, Norcross, GA), SHH peptide was quantified using the Mouse Shh-N ELISA Kit (#RAB0431, Sigma-Aldrich, St. Louis, MO), IFN- γ levels were determined

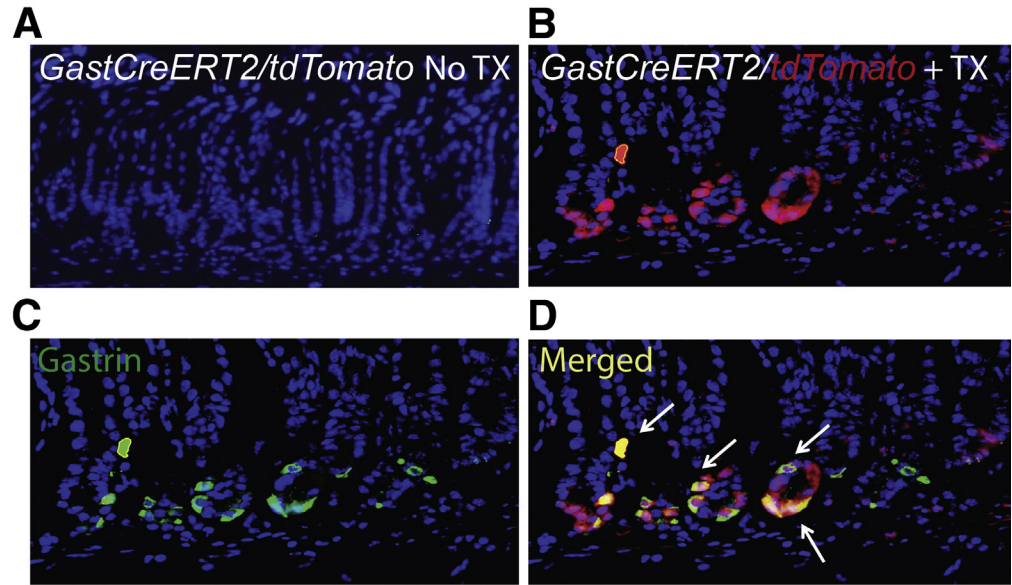


Figure 10. Characterization of *GastCreERT2* transgenic line. *GastCreERT2/tdTomato* mouse showing (A) no tdTomato expression without TX treatment and (B) tdTomato (red) expression at the base of antral glands after 2 months of TX treatment activates Cre recombinase. Immunostaining for (C) gastrin (green) colocalized with (D) cells expressing tdTomato in the antrum of *GastCreERT2/tdTomato* mice (arrows, colocalization).

using the Mouse IFN- γ ELISA Kit (Thermo Fisher, #EM1001), and IL1 β levels were determined using the Mouse ELISA kit (#197742, Abcam, Cambridge, UK) or the human ELISA kit for hIL1 β transgene expression (Abcam, #100562), per the manufacturer's instructions. Serum was diluted 1:8 fold with dilution buffer for ELISA.

Histologic Analysis

Five micron sections were prepared, deparaffinized, and then rehydrated. Each slide contained sections of well-oriented gastric glandular mucosa that extended along the greater curvature of the stomach. Slides were stained with hematoxylin and eosin for histology. Specific protein expression was identified by immunofluorescent staining. Antigen retrieval was performed using 10 mM citrate (pH 6). Slides were washed twice in phosphate-buffered saline containing 0.01% Triton X-100, incubated for 1 hour with the serum of the animal in which the secondary antibody was raised. Next, slides were incubated with the following antibodies overnight: Gastrin (DAKO, #A0568), Ki67 (Abcam, #15580), hIL1 β (#10139-M201, Sino Biological, North Wales, PA), mIL1 β (R&D, AF-401-NA), mIFN- γ

(Interferon Source, #22100-3), Acetylated Tubulin (Sigma, #MABT868), and E-Cadherin (BD, #51-9001922). Alexa Fluor-conjugated secondary antibodies (Molecular Probes, Eugene, OR; Invitrogen, Carlsbad, CA) were used to detect primary antibodies at a dilution of 1:500. Slides were mounted with Prolong gold anti-fade reagent with DAPI (Life Technologies, Rockville, MD). Immunofluorescence was visualized using the Nikon Eclipse E800 microscope (Nikon, Tokyo, Japan) or Olympus BX53F (Center Valley, PA).

Gastric Acid Determination

Stomachs were resected and opened along the greater curvature. The gastric content was collected in 1.5 mL of 0.9% NaCl (pH 7.0) following centrifugation (1700 $\times g$ for 5 minutes) to collect a clear supernatant. The hydrogen ion concentration was determined by titrating with 0.005 N sodium hydroxide using a pH meter (Orion Star A111) and then normalized to the stomach weight.

Real-time Quantitative Polymerase Chain Reaction

Total RNA was extracted from freshly collected stomach tissue or GLUTag cells in TRIzol (Invitrogen). The RNeasy Minikit (Qiagen, Valencia, CA) was used to extract total RNA. RNA (1 μ g) was DNase-treated (Promega, Fitchburg, WI) before generating complementary DNA using the iScript reverse transcriptase (Bio-Rad, Hercules, CA). Real-time qPCR was performed using Platinum Taq DNA polymerase (Invitrogen) on a CFX96 real-time PCR detection system (Bio-RAD), using the following primer sequences (Tm = 65°C for all primers):

Gast-F: 5'ACACAACAGCCAACTATTC-3', R: 5'-CAAAGTC-CATCCATCCGTAG-3'

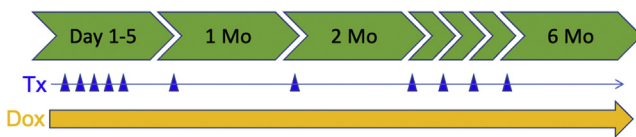


Figure 11. Outline of treatment protocol for inducing IFN- γ or IL1 β in *GastCreERT2/TetOn-mIrfn γ* and *GastCreERT2/TetOn-hIL-1 β* mice. WT and transgenic mice were intraperitoneally injected with TX (0.2 mg/g body weight) for 5 consecutive days and then received 1 injection each of the following months. DOX (2 mg/mL) was administered from the beginning in the drinking water every day until euthanized at 6 months.

Gli1-F: 5'-TTGGGATGAAGAAGCAGTTG-3' R: 5'-GGAGA-CAGCATGGCTCACTA-3';

Gli2-F: 5'-ACCCAACACTCAGCAGCAGTAGC-3' R: 5'-GCTCCGCTTATGAATGGTGATGG-3';

HPRT-F: 5'-AGGACCTCTCGAAGTGTGGATAC-3' R: 5'-AACTTGGCCTCATCTTAGGCTTTG-3'. Gene expression was normalized to *HPRT*, and fold changes were calculated using the $2^{-\Delta\Delta CT}$ method.³⁸

Western Blot Analysis

Gastric tissue was homogenized in RIPA buffer (Pierce, Rockford, IL). Western blots were performed using the SDS-PAGE System. Briefly, 20 μ g of protein were resuspended in sample buffer, then electrophoresed on Novex 4–20% Tris-Glycine gels (Invitrogen) with Tris running buffer; transferred to PVDF membrane using the iBlot Dry Blotting System (Invitrogen) according to the manufacturer's instructions. The membranes were incubated in 5% nonfat milk for 1 hour at room temperature and then sequentially probed with primary antibodies to *GLI2* (#sc271786, Santa Cruz Biotechnology, Dallas, TX), *KIF3A* (Abcam, #11256), or *GAPDH* (Thermo Fisher, #MA5-15738) overnight at 4°C.

Flow Cytometry

The antrum was minced, incubated in 20 mL of collagenase (1.5 mg/mL Type VIII Collagenase) dissolved in prewarmed CMF HBSS/fetal bovine serum with 40 μ g/mL of DNase I for digestion at 200 rpm for 20 min at 37°C. After passing through the 100- μ m cell strainer and centrifuging at 1500 rpm for 5 min at 4°C, the cell pellet was resuspended in phosphate-buffered saline containing 5% bovine serum albumin. Cell suspensions were blocked with purified rat anti-mouse DC16/CD32 mouse Fc block (BD Biosciences) at 4°C for 5 minutes, before incubating with IL1 β -PE (#12-7114-80, eBioscience) and CD45-FITC (#50-163-420, Thermo Fisher). Before staining for intracellular protein E-cadherin (SC7870, Santa Cruz), cells were fixed and permeabilized with Fix and Perm Kit (Thermo Fisher). Fluorescent conjugated secondary antibodies were purchased from Life Technologies. The cells were analyzed on a BD FACSCanto II system (BD Biosciences).

Statistical Analysis

For cilium length quantitation, significance was determined using Kruskal-Wallis analysis of variance with Dunn test for multiple comparisons. Significance for all in vivo mouse experiments, ELISAs, and qPCR mRNA was determined using 2-way analysis of variance with Geisser-Greenhouse correction. For ELISAs and qPCR determinations in the cell culture experiments, significance was performed on the log-transformed values using 1-way analysis of variance with Tukey post hoc test for multiple comparisons.

References

1. Banks M, Graham D, Jansen M, Gotoda T, Coda S, di Pietro M, Uedo N, Bhandari P, Pritchard DM, Kuipers EJ, Rodriguez-Justo M, Novelli MR, Ragnunath K, Shepherd N, Dinis-Ribeiro M. British Society of Gastroenterology guidelines on the diagnosis and management of patients at risk of gastric adenocarcinoma. *Gut* 2019; 68:1545–1575.
2. Shang J, Pena AS. Multidisciplinary approach to understand the pathogenesis of gastric cancer. *World J Gastroenterol* 2005;11:4131–4139.
3. Merchant JL, Ding L. Hedgehog signaling links chronic inflammation to gastric cancer precursor lesions. *Cell Mol Gastroenterol Hepatol* 2017;3:201–210.
4. Waghray M, Zavros Y, Saqui-Salces M, El-Zaatari M, Alamelumangapuram CB, Todisco A, Eaton KA, Merchant JL. Interleukin-1beta promotes gastric atrophy through suppression of sonic hedgehog. *Gastroenterology* 2010;138:562–572.
5. El-Omar EM, Carrington M, Chow WH, McColl KE, Bream JH, Young HA, Herrera J, Lissowska J, Yuan CC, Rothman N, Lanyon G, Martin M, Fraumeni JF Jr, Rabkin CS. Interleukin-1 polymorphisms associated with increased risk of gastric cancer. *Nature* 2000; 404:398–402.
6. Zavros Y, Rathinavelu S, Kao JY, Todisco A, Del Valle J, Weinstock JV, Low MJ, Merchant JL. Treatment of *Helicobacter* gastritis with IL-4 requires somatostatin. *Proc Natl Acad Sci U S A* 2003;100:12944–12949.
7. Tu S, Bhagat G, Cui G, Takaishi S, Kurt-Jones EA, Rickman B, Betz KS, Penz-Oesterreicher M, Bjorkdahl O, Fox JG, Wang TC. Overexpression of interleukin-1beta induces gastric inflammation and cancer and mobilizes myeloid-derived suppressor cells in mice. *Cancer Cell* 2008;14:408–419.
8. Syu LJ, El-Zaatari M, Eaton KA, Liu Z, Tetarbe M, Keeley TM, Pero J, Ferris J, Wilbert D, Kaatz A, Zheng X, Qiao X, Grachtchouk M, Gumucio DL, Merchant JL, Samuelson LC, Dlugosz AA. Transgenic expression of interferon-gamma in mouse stomach leads to inflammation, metaplasia, and dysplasia. *Am J Pathol* 2012; 181:2114–2125.
9. Gupta S, Tao L, Murphy JD, Camargo MC, Oren E, Valasek MA, Gomez SL, Martinez ME. Race/ethnicity-, socioeconomic status-, and anatomic subsite-specific risks for gastric cancer. *Gastroenterology* 2019; 156:59–62.
10. O'Connor A, Bowden A, Farrell E, Weininger J, Crowther S, McNamara D, Ridgway P, O'Morain C. Risk of progression of gastric intestinal metaplasia is significantly greater when detected in both antrum and body. *Dig Dis Sci* 2020.
11. Merchant JL. Inflammation, atrophy, gastric cancer: connecting the molecular dots. *Gastroenterology* 2005; 129:1079–1082.
12. Shiotani A, Iishi H, Uedo N, Ishiguro S, Tatsuta M, Nakae Y, Kumamoto M, Merchant JL. Evidence that loss of sonic hedgehog is an indicator of *Helicobacter pylori*-induced atrophic gastritis progressing to gastric cancer. *Am J Gastroenterol* 2005;100:581–587.
13. Zavros Y, Eaton KA, Kang W, Rathinavelu S, Katukuri V, Kao JY, Samuelson LC, Merchant JL. Chronic gastritis in the hypochlorhydric gastrin-deficient mouse progresses to adenocarcinoma. *Oncogene* 2005;24:2354–2366.

14. Soutto M, Belkhir A, Piazuolo MB, Schneider BG, Peng D, Jiang A, Washington MK, Kokoye Y, Crowe SE, Zaika A, Correa P, Peek RM Jr, El-Rifai W. Loss of TFF1 is associated with activation of NF-kappaB-mediated inflammation and gastric neoplasia in mice and humans. *J Clin Invest* 2011;121:1753–1767.
15. Ramalho-Santos M, Melton DA, McMahon AP. Hedgehog signals regulate multiple aspects of gastrointestinal development. *Development* 2000;127:2763–2772.
16. Kolterud A, Grosse AS, Zacharias WJ, Walton KD, Kretovich KE, Madison BB, Waghray M, Ferris JE, Hu C, Merchant JL, Dlugosz AA, Kottmann AH, Gumucio DL. Paracrine hedgehog signaling in stomach and intestine: new roles for hedgehog in gastrointestinal patterning. *Gastroenterology* 2009;137:618–628.
17. Syu LJ, Zhao X, Zhang Y, Grachtchouk M, Demitrack E, Ermilov A, Wilbert DM, Zheng X, Kaatz A, Greenson JK, Gumucio DL, Merchant JL, di Magliano MP, Samuelson LC, Dlugosz AA. Invasive mouse gastric adenocarcinomas arising from Lgr5+ stem cells are dependent on crosstalk between the hedgehog/GLI2 and mTOR pathways. *Oncotarget* 2016;7:10255–10270.
18. Saqui-Salces M, Coves-Datson E, Veniaminova NA, Waghray M, Syu LJ, Dlugosz AA, Merchant JL. Inflammation and Gli2 suppress gastrin gene expression in a murine model of antral hyperplasia. *PLoS One* 2012;7:e48039.
19. Bangs F, Anderson KV. Primary cilia and mammalian hedgehog signaling. *Cold Spring Harb Perspect Biol* 2017;9:a028175.
20. Saqui-Salces M, Dowdle WE, Reiter JF, Merchant JL. A high-fat diet regulates gastrin and acid secretion through primary cilia. *FASEB J* 2012;26:3127–3139.
21. Wann AK, Knight MM. Primary cilia elongation in response to interleukin-1 mediates the inflammatory response. *Cell Mol Life Sci* 2012;69:2967–2977.
22. Hassounah NB, Bunch TA, McDermott KM. Molecular pathways: the role of primary cilia in cancer progression and therapeutics with a focus on hedgehog signaling. *Clin Cancer Res* 2012;18:2429–2435.
23. Zavros Y, Rieder G, Ferguson A, Merchant JL. Gastritis and hypergastrinemia due to *Acinetobacter Iwoffii* in mice. *Infect Immun* 2002;70:2630–2639.
24. Ding L, Hayes MM, Photenhauer A, Eaton KA, Li Q, Ocadiz-Ruiz R, Merchant JL. Schlafen 4-expressing myeloid-derived suppressor cells are induced during murine gastric metaplasia. *J Clin Invest* 2016;126:2867–2880.
25. El-Zaatari M, Zavros Y, Tessier A, Waghray M, Lentz S, Gumucio D, Todisco A, Merchant JL. Intracellular calcium release and protein kinase C activation stimulate sonic hedgehog gene expression during gastric acid secretion. *Gastroenterology* 2010;139:2061–2071.
26. Xiao C, Ogle SA, Schumacher MA, Orr-Asman MA, Miller ML, Lertkowitz N, Varro A, Hollande F, Zavros Y. Loss of parietal cell expression of sonic hedgehog induces hypergastrinemia and hyperproliferation of surface mucous cells. *Gastroenterology* 2010;138:550–561.
27. Delling M, DeCaen PG, Doerner JF, Febvay S, Clapham DE. Primary cilia are specialized calcium signalling organelles. *Nature* 2013;504:311–314.
28. Santos N, Reiter JF. A central region of Gli2 regulates its localization to the primary cilium and transcriptional activity. *J Cell Sci* 2014;127(Pt 7):1500–1510.
29. Wann AK, Thompson CL, Chapple JP, Knight MM. Interleukin-1beta sequesters hypoxia inducible factor 2alpha to the primary cilium. *Cilia* 2013;2:17.
30. Wann AK, Chapple JP, Knight MM. The primary cilium influences interleukin-1beta-induced NFkappaB signaling by regulating IKK activity. *Cell Signal* 2014;26:1735–1742.
31. Fox JG, Wang TC. Inflammation, atrophy, and gastric cancer. *J Clin Invest* 2007;117:60–69.
32. Fu S, Thompson CL, Ali A, Wang W, Chapple JP, Mitchison HM, Beales PL, Wann AKT, Knight MM. Mechanical loading inhibits cartilage inflammatory signalling via an HDAC6 and IFT-dependent mechanism regulating primary cilia elongation. *Osteoarthritis Cartilage* 2019;27:1064–1074.
33. Besschetnova TY, Kolpakova-Hart E, Guan Y, Zhou J, Olsen BR, Shah JV. Identification of signaling pathways regulating primary cilium length and flow-mediated adaptation. *Curr Biol* 2010;20:182–187.
34. Canterini S, Dragotto J, Dardis A, Zampieri S, De Stefano ME, Mangia F, Erickson RP, Fiorenza MT. Shortened primary cilium length and dysregulated sonic hedgehog signaling in Niemann-Pick C1 disease. *Hum Mol Genet* 2017;26:2277–2289.
35. El-Zaatari M, Kao JY, Tessier A, Bai L, Hayes MM, Fontaine C, Eaton KA, Merchant JL. Gli1 deletion prevents *Helicobacter*-induced gastric metaplasia and expansion of myeloid cell subsets. *PLoS One* 2013;8:e58935.
36. Marszalek JR, Ruiz-Lozano P, Roberts E, Chien KR, Goldstein LS. Situs inversus and embryonic ciliary morphogenesis defects in mouse mutants lacking the KIF3A subunit of kinesin-II. *Proc Natl Acad Sci U S A* 1999;96:5043–5048.
37. Lee YC, Asa SL, Drucker DJ. Glucagon gene 5'-flanking sequences direct expression of simian virus 40 large T antigen to the intestine, producing carcinoma of the large bowel in transgenic mice. *J Biol Chem* 1992;267:10705–10708.
38. Schmittgen TD, Livak KJ. Analyzing real-time PCR data by the comparative C(T) method. *Nat Protoc* 2008;3:1101–1108.

Received June 19, 2020. Accepted December 11, 2020.

Correspondence

Address correspondence to: Juanita L. Merchant, MD, PhD, 1501 North Campbell Avenue, PO Box 245028, Tucson, Arizona 85724-5028. e-mail: jmerchant@email.arizona.edu; fax: (520) 626-2520.

CRedit Authorship Contributions

Lin Ding (Data curation: Lead; Formal analysis: Lead; Methodology: Lead; Supervision: Supporting; Validation: Lead; Writing – original draft: Lead; Writing – review & editing: Equal)

Ricky A. Sontz (Data curation: Supporting; Methodology: Supporting)

Milena Saqui-Salces (Data curation: Supporting; Investigation: Supporting; Resources: Supporting; Validation: Supporting; Writing – review & editing: Equal)

Juanita L. Merchant, MD, PhD (Conceptualization: Lead; Funding acquisition: Lead; Methodology: Equal; Project administration: Lead;

Resources: Lead; Supervision: Lead; Writing – original draft: Equal; Writing – review & editing: Lead)

Conflicts of interest

The authors disclose no conflicts.

Funding

Supported by R01 DK118563 and P01 DK062041 (to JLM), R01 DK45729 to JLM and Arizona Comprehensive Cancer Center P30 CA023074 and University of Michigan Digestive Disease Center P30 DK034933.